First-Principles Study of Cubic $B_xIn_{1-x}N$ Ternary Alloys

A. Abdiche[a], H. Abid[a], R. Riane[b] and A. Bouaza[c]

[a]Applied Materials Laboratory, University Research of Sidi-Bel-Abbes, 22000, Algeria

[b]Computational Materials Science Laboratory, University Research of Sidi-Bel-Abbes, 22000, Algeria

[c]Engineering Physics Laboratory, University Research of Tiaret, 14000, Algeria

(Received October 28, 2009; revised version November 24, 2009; in final form January 10, 2010)

We present first principles calculations of the structural and electronic properties of zinc blende BN, InN and their ternary alloy $B_xIn_{1-x}N$ for concentrations $x = 0.25$, 0.5, 0.75. The computational method used is based on the full potential linearized augmented plane wave. The exchange and correlation energy is described in the local density approximation and generalized gradient approximation. We have studied the structural and electronic properties. First, the lattice constants a_0, bulk modulus B, pressure derivative B' for zinc blende BN, InN, and $B_xIn_{1-x}N$ solid solutions were carried out. Thereafter, the band gap energies and the densities of states of binary compounds and the ternary alloy $B_xIn_{1-x}N$ were investigated. Results obtained and compared with available experimental and theoretical values show a reasonable agreement.

PACS numbers: 61.50.ks, 64.70.Rb, 71.15.Mb

1. Introduction

III–V and II–IV semiconductors are the most studied today and constitute the basic building blocks of emitters and receivers in optoelectronic devices. Group-III nitrides are nowadays widely used in the industry. With respect to classical III–V semiconductors, the group-III nitrides semiconductors have attracted much attention in recent years due to their great potential for optoelectronic applications [1]. In this study, first principles total energy calculations were carried out to investigate structural and electronic properties of ternary alloys $B_xIn_{1-x}N$, binary compounds BN and InN.

On the theoretical side, the binary BN, AlN, GaN, InN [2–4] and their solid solutions BGaN, BAlN, AlInN [4, 5] were carried out using different methods in the calculation of the band structure of these alloys. These include methods based on the dielectric two-band model [6], semi-empirical tight-binding method [7, 8] semi-empirical pseudo-potential method [9, 10], *ab initio* pseudo-potential method [11–22] and full potential linearized augmented plane wave (FP-LAPW) method [23, 24]. To our knowledge, there is no theoretical investigation of $B_xIn_{1-x}N$ alloy. To understand the structural and electronic properties of these ternary alloys, we carry out the present study, in which we have used the first principles FP-LAPW method within the local density approximation (LDA) and generalized gradient approximation (GGA) scheme [25–27].

2. Calculation method

In this work we used the scalar nonrelativistic full potential linearized augmented plane wave plus local orbital (FP-L/APW+LO) [28] approach based on the density functional theory [29] within the LDA and GGA using the scheme of Perdew et al. [30]. The exchange correlation energy was parameterized by Perdew and Wang [31].

In the present calculations we apply the most recent version of Vienna package WIEN2k [32, 33]. In this new version, the alternative base sets (APW+LO) are used inside the atomic spheres for those chemically important l-orbital (partial waves) that converge with difficulty (outermost valence p, d, or f-states), or for atoms where small atomic spheres must be used [34, 35]. For all the other partial waves, the LAPW scheme is used.

Moreover, we used the semi-relativistic approximation (no spin–orbit effects included) whereas the core levels are treated fully nonrelativistically [36]. In particular, the indium is considered to include explicitly the semicore d electrons in the valence bands. In the following calculations, we distinguish the B ($1s^2$), In ($1s^2$ $2s^2$ $2p^6$ $3s^2$ $3p^6$ $3d^{10}$ $4s^2$ $4p^6$), and N ($1s^2$) inner-shell electrons from the valence electrons of B ($2s^2$ $2p^1$), In ($4d^{10}$ $5s^2$ $5p^1$) and N ($2s^2$ $2p^3$) shells.

The core states are self-consistently relaxed in a spherical approximation. Inside the non-overlapping spheres of muffin-tin (MT) radius R_{MT} (bohr) around each atom, spherical harmonic expansion is used. We chose the plane wave basis set for the remaining space of the unit cell. For BN and InN we adopted as the MT radius, the values of 1.5, 2.4, and 1.4 for B, In, and N, respectively. The max-

imum l value for the wave function expansion inside the atomic spheres was confined to $l_{\max} = 10$. In order to achieve energy eigenvalues convergence, the wave functions in the interstitial region are expanded into plane waves with a cutoff of $R_{\mathrm{MT}}k_{\mathrm{MAX}} = 7$ (where k_{MAX} is the maximum reciprocal lattice vector, and R_{MT} is the average radius of the MT spheres). The k integration over the Brillouin zone is performed using Monkhorst and Pack [37] mesh, yielding to $27k$ points in the irreducible wedge of the Brillouin zone for both zinc blende structures. In ternary semiconductor alloys, the optical bowing is a well known phenomenon. This bowing in large band gap of III–V semiconductor has been observed more than thirty years ago by Larach et al. [38] on powder material and by Ebina et al. [39].

The k integration over Brillouin zone is performed using tetrahedron method [40].

3. Results and discussions

3.1. Structural properties

The structural properties of the binary compounds BN and InN in the zinc-blende structure were carried out using the FP-LAPW method. We have chosen the basic cubic cell as the unit cell. For the considered structures, zinc blende (ZB) BN and InN, we performed the structural optimization by calculating the total energies for different volumes around the equilibrium cell volume V_0 of the binary BN and InN compounds and their alloys. The calculated total energies are fitted to the Murnaghan equation of state to determine the ground state properties as the equilibrium lattice constant a_0, the bulk modulus B_0 and its pressure derivative B'. The calculated equilibrium parameters (a_0, B, and B') and other available experimental and calculated values are summarized in Table I. A good agreement is found. Also, there is a small underestimation of the lattice parameters and overestimations of the bulk modulus compared to the experimental data; this is due essentially to the use of the LDA and GGA. Furthermore, the values of the calculated bulk modulus (in LDA) approximation decrease from BN to InN, i.e. from the lower to the higher atomic number. This suggests that BN is less compressible than InN.

TABLE I

Lattice constants a, bulk modulus B, and pressure derivative B' for ZB InN, BN and $B_xIn_{1-x}N$ solid solutions.

Composition		This work		Other theoretical studies	Experimental data
		LDA	GGA		
InN	a [Å]	4.98	5.08	5.04–4.94[a]	4.98[h]
	B [GPa]	155.35	127.71	133–146[a]	137[i]
	B' [GPa]	4.49	3.40	3.36–4.48[a]	
$B_{0.25}In_{0.75}N$	a [Å]	4.83	4.91		
	B [GPa]	173.85	153.00		
	B' [GPa]	3.65	3.91		
$B_{0.5}In_{0.5}N$	a [Å]	4.56	4.61		
	B [GPa]	199.56	182.86		
	B' [GPa]	3.51	3.55		
$B_{0.75}In_{0.25}N$	a [Å]	4.21	4.26		
	B [GPa]	403.86	257.98		
	B' [GPa]	3.42	3.48		
BN	a [Å]	3.58	3.63	3.60, 3.57[b], 3.57–3.64[c]	3.61[d]
	B [GPa]	408.89	395.74	367, 386[b], 397–366[c]	369[e]
	B' [GPa]	3.65	2.94	3.94[f], 3.6, 2.91–3.97[g]	4.1[f], 3.0–4.0[g]

[a]Ref. [49]; [b]Ref. [14–16]; [c]Ref. [20, 21]; [d]Ref. [17, 18]; [e]Ref. [17]; [f]Ref. [13]; [g]Ref. [20–22]; [h]Ref. [54]; [i]Ref. [55]

Usually, in the treatment of alloys, it is assumed that the atoms are located at the ideal lattice sites and the lattice constant varies linearly with composition x according to the so-called Vegard law [41]:

$$a(A_xB_{1-x}C) = xa_{AC} + (1-x)a_{BC}\,, \qquad (1)$$

where a_{AC}, a_{BC} are the equilibrium lattice constants of

the binary compounds AC and BC, respectively, and $a(A_xB_{1-x}C)$ is the alloy lattice constant. However, violation of Vegard's law has been observed in semiconductor alloys both experimentally [42] and theoretically [43, 44]. Hence, the lattice constant can be written as

$$a(A_xB_{1-x}C) = xa_{AC} + (1-x)a_{BC} - x(1-x)b\,, \quad (2)$$

where the quadratic term b is the bowing parameter.

Figures 1 and 2 show the variation of the calculated equilibrium lattice constants and the bulk modulus versus concentration x_B for $B_xIn_{1-x}N$ alloy, respectively. It is very clear from Fig. 2 that the value of the bulk modulus increase with increasing x_B concentration. To analyze the degree of deviation from the Vegard law, the lattice constant of $B_xIn_{1-x}N$ solid solutions as a function of the boron composition x can be approximated using the formula (2):

$$a(x) = xa_{BN} + (1-x)a_{InN} - x(1-x)b\,. \quad (3)$$

With the best fit of results shown in Fig. 1, using Eq. (3) we found the deviation parameter of the lattice constant $b = -1.1$. This result can be explained by the use of LDA and GGA approximations to simulate the ternary $B_xIn_{1-x}N$ within an ordered supercell. It is clearly known that both LDA and GGA underestimate physical parameters. We note that solid solution assuming disorder can be better carried out using coherent potential approximation (CPA) [45].

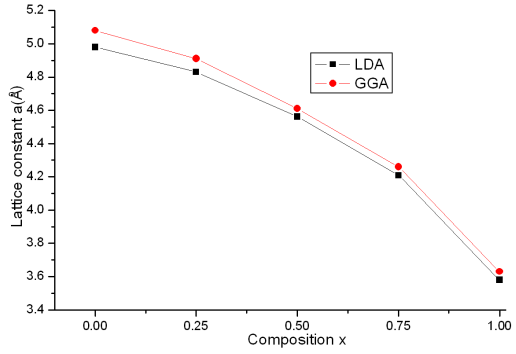

Fig. 1. Lattice constant of $B_xIn_{1-x}N$ alloys.

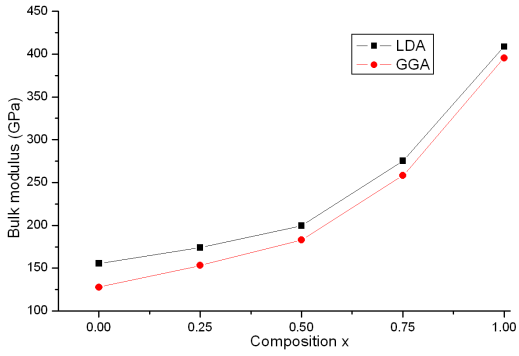

Fig. 2. Bulk modulus of $B_xIn_{1-x}N$ alloys.

3.2. Electronic properties

Figures 3 and 4 show the calculated band structure energies of binary compounds BN and InN. We have ob-

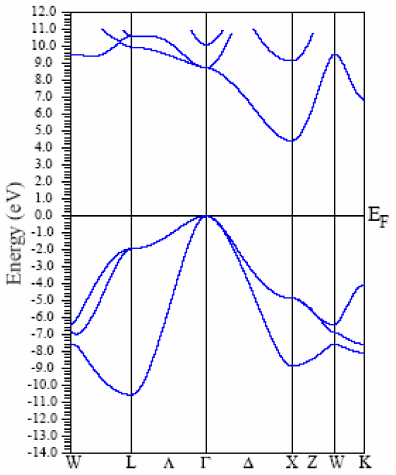

Fig. 3. Band structure of ZB BN.

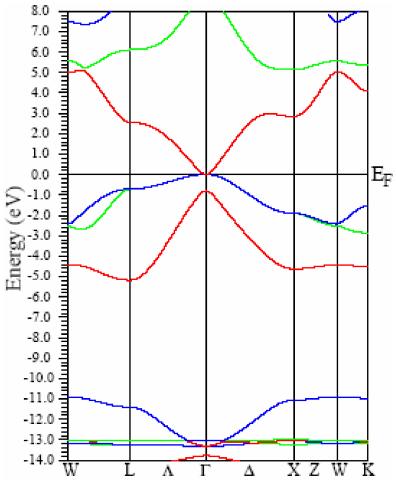

Fig. 4. Band structure of ZB InN.

tained an indirect band gap for the BN with a value of 8.67 eV and a direct band gap for the InN with a value of 0.0 eV. The band gap calculated for the ZB InN using the LDA or GGA approximations describes InN as metallic compound. Using the exchange potential of Engel and Vosko [46] a semiconductor phase is found for both crystal structures, although the band gap is underestimated. The band gap has been improved according to a quasi-particle correction. However, it has been shown by Del Sole and Girlanda [47] that the LDA combined with the scissors-operator approximation describes the optical spectrum rather well. The correct value for the InN band gap can be calculated by using the quasi-particle method proposed by Bechstedt and Sole [48]. This model for the correction is based on the difference in

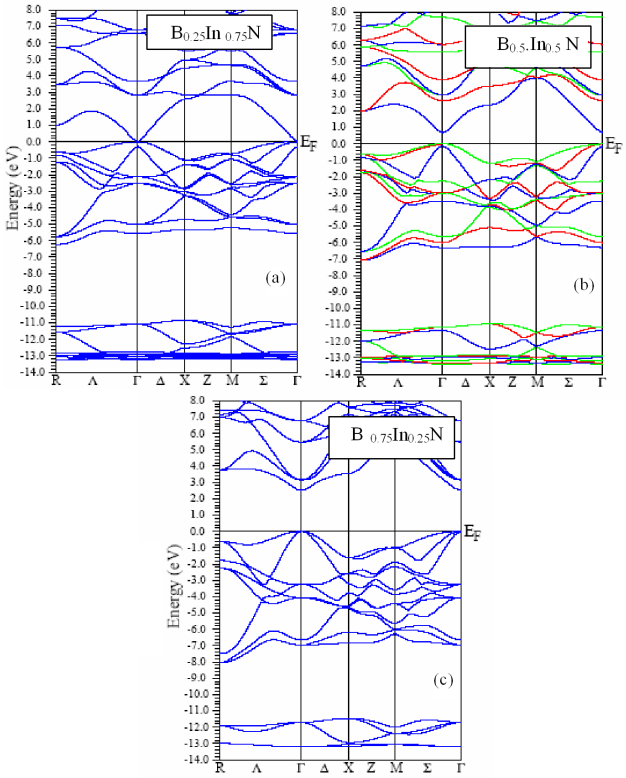

Fig. 5. The band structure of ZB ternary alloy $B_xIn_{1-x}N$: (a) $x = 0.25$, (b) $x = 0.5$, (c) $x = 0.75$.

self-energies obtained from the LDA and the GW approximation. Focusing now on the $B_xIn_{1-x}N$ solid solutions, our calculations give direct band gaps with different compositions x ($x = 0.25$, 0.5, 0.75). The results are reported in Fig. 5 a–c. The main band gaps are given in Table II, as well as the available theoretical and experimental values.

It is clearly seen that the band gaps are on the whole underestimated in comparison with experimental results. This underestimation of the band gaps is mainly due to the fact that the simple form of GGA does not take into account the quasiparticle self-energy correctly which make it not sufficiently flexible to accurately reproduce both exchange correlation energy and its charge derivative. It is important to note that the density functional formalism is limited in its validity and the band structure derived from it cannot be used directly for comparison with experiment.

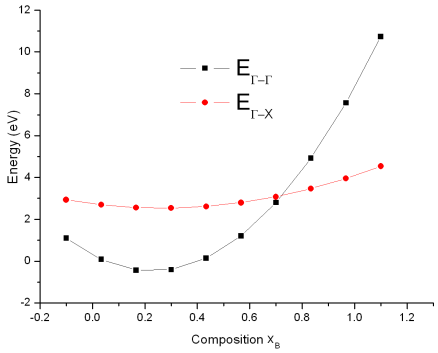

Fig. 6. Composition dependence of the direct (Γ–Γ) and indirect (Γ–X) band gaps in $B_xIn_{1-x}N$ alloys.

The variation of the direct $E_{\Gamma-\Gamma}$ and indirect $E_{\Gamma-X}$ band gaps versus alloy composition is given in Fig. 6. A crossover between the direct and indirect band gaps is located at a concentration of 0.719. We note that the fundamental gap $E_{\Gamma-\Gamma}$ increases considerably with the boron composition, but only a small increase is seen for the indirect gap $E_{\Gamma-X}$. The bowing parameter is calculated by fitting the non-linear variation of the calculated direct and indirect band gaps in terms of concentration with polynomial function. The results are shown in Fig. 6 and obey the following variations:

$$E_{\Gamma-\Gamma} = 0.287 - 6.73x + 14.75x^2, \quad (4)$$

$$E_{\Gamma-X} = 2.899 - 1.55x + 2.899x^2. \quad (5)$$

It is shown from the above equations that variation of direct $E_{\Gamma-\Gamma}$ and indirect $E_{\Gamma-X}$ band gaps as a function of concentration has a non-linear behavior. The direct gap $E_{\Gamma-\Gamma}$ versus concentration has a large bowing with a value of $b = 14.75$, while the indirect gap $E_{\Gamma-X}$ has a bowing of $b = 2.899$. The values of these bowings are close to those obtained by using the FP-LAPW method.

TABLE II

Direct (Γ–Γ) and indirect (Γ–X) band gaps for zinc blende InN, BN and their alloys $B_xIn_{1-x}N$.

Composition	This work GGA		Other theoretical studies	Experimental data
	$E_{\Gamma-\Gamma}$	$E_{\Gamma-X}$		
InN	0.00	2.765	0.00[a], 0.15[d], 0.69[g]	2.11[d], 1.9[f]
$B_{0.25}In_{0.75}N$	0.0208	2.597	–	–
$B_{0.5}In_{0.5}N$	0.855	2.362	–	–
$B_{0.75}In_{0.25}N$	2.716	3.582	–	–
BN	8.677	3.955	9.09–4.24[b], 8.79–4.45[c]	6[e]

[a]Ref. [50]; [b]Ref. [49]; [c]Ref. [51]; [d]Ref. [46]; [e]Ref. [52]; [f]Ref. [53]

The shift between the lattice parameters of BN and InN is larger than 20%. This can induce an important disorder which affects the electronic and structural properties. The ternary $B_xIn_{1-x}N$ shows a direct gap for the compositions $x = 0.25$, 0.5, and 0.75. The boron fraction modulates the gap energy: from 0.022 eV (for $x = 0.25$ to 2.71 eV for $x = 0.75$). The band gap energy increases considerably with high boron composition x. The $B_{0.75}In_{0.25}N$ is a wide gap semiconductor.

3.3. Density of states (DOS)

The essential ingredient in determining the electronic properties of solids is the energy distribution of the valence and band electrons. Theoretical quantities such as

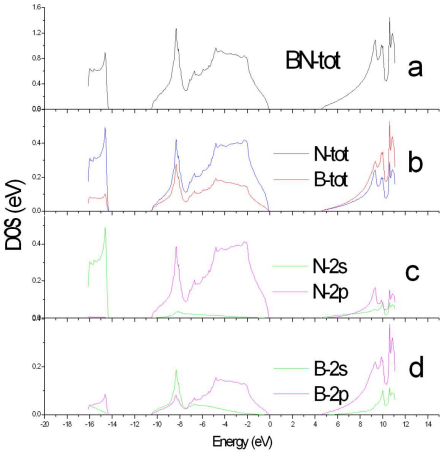

Fig. 7. Total density of state of BN (a) and angular--momentum decomposition of the atom-project densities of states in c-BN (b)–(d).

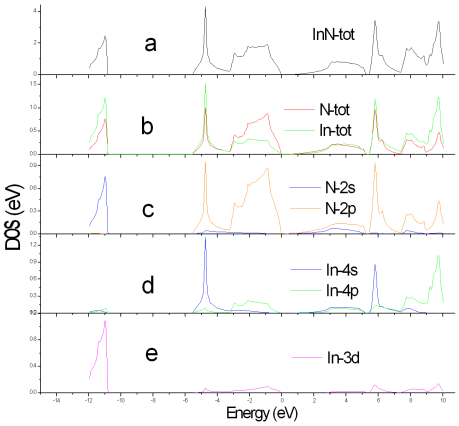

Fig. 8. Total density of state of InN (a) and angular--momentum decomposition of the atom-project densities of states in c-InN (b)–(e).

total electronic energy of solid, the position of the Fermi level and tunneling probabilities of electrons call for detailed calculation of electronic density of states. Calculation of the DOS requires a very high degree of precision

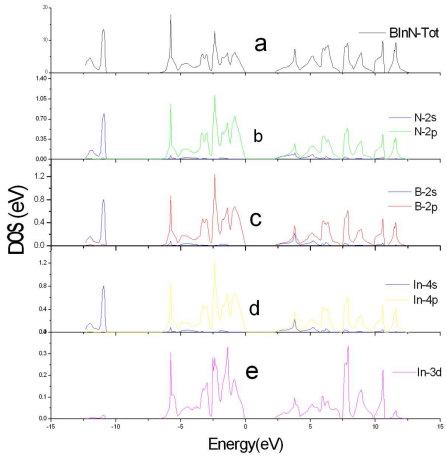

Fig. 9. Total density of state of $B_{0.75}In_{0.25}N$ (a) and angular momentum decomposition of the atom-project densities of states in c-$B_{0.75}In_{0.25}N$ (b)–(e).

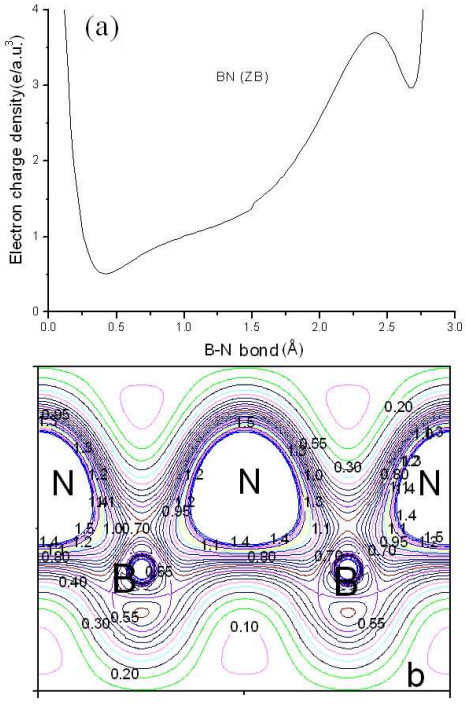

Fig. 10. Total valence charge densities in zinc blende BN: (a) along (111) direction, (b) in the (110) plane.

with the use of a fine k-point mesh in the first Brillouin zone (BZ). In our calculations we considered a k-mesh = 3000 for binary compounds BN and InN and a k-mesh = 60 for the $B_{0.75}In_{0.25}N$ solid solution. For ZB InN and BN the total DOS presents three regions: two valence regions VB1, VB2 and one conduction band CB. Figures 7a and 8a show the partial and total DOS for the BN and InN. For BN the lower VB2 valence band region is dominated by N $2s$ states, and the upper VB1 valence band by N $2p^3$ and B $2s$. The conduction band results from

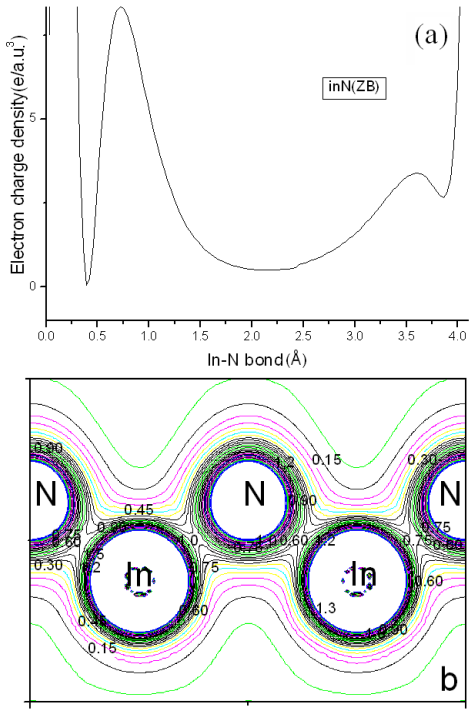

Fig. 11. Total valence charge densities in zinc blende InN: (a) along (111) direction, (b) in the (110) plane.

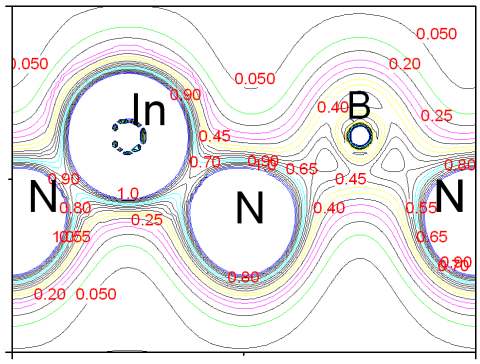

Fig. 12. Total valence charge densities in zinc blende $B_{0.75}In_{0.25}N$ along (110) plane.

the contribution of N 2p and B 2p. For the InN the VB2 is dominated by N 2s and In 3d states. The In 4s and N 2p states contribute to the upper valence bands. The first conduction band is predominantly of N 2p states. The total DOS of $B_{0.75}In_{0.25}N$ shown in Fig. 9a is essential to study the nature of chemical bonding in this material. In this case the total DOS presents three regions, the first region is dominated by N 2s and In 4s, the second region results from the contributions of N 2p, B 2p and In 4p states. The In 3d states contribute in the third region. The charge transfer from boron to nitrogen is due to the difference in electronegativity between nitrogen and boron and explains the occurrence of the first peak in B0.75 In0.25 N. Figures 10a, 11a show the electronic densities for the ZB BN and InN in the (111) direction. Figures 10b, 11b and 12 present the contour plot for BN, InN and $B_{0.75}In_{0.25}N$ in the plane (110).

4. Conclusion

We have used the FP-LAPW method within the LDA and GGA approximations to investigate the structural and electronic properties of the cubic $B_xIn_{1-x}N$ alloy. We have calculated the equilibrium lattice constants, bulk modulus, and pressure derivatives. The bowings of the lattice constant, bulk modulus and energy band gap are also investigated. The $B_xIn_{1-x}N$ for the composition $x = 0.75$ is a wide gap semiconductor and may be a good material for optoelectronic industry. The results show a strong dependence of the band gap bowing factor on composition of boron x.

References

[1] H. Okuyama, T. Miyajima, Y. Morinaga, F. Hiei, M. Ozawa, K. Akimot, *Electron. Lett.* **28**, 1798 (1992).

[2] S. Strite, H. Morkoc, *J. Vac. Sci. Technol. B* **10**, 1237 (1992).

[3] R.F. Davis, Z. Sitar, B.E. Williams, H.S. Kong, H.J. Kim, J.W. Palmour, J.A. Edmond, J. Ryu, J.T. Glas, C.H. Carter Jr, *Mater. Sci. Eng. B* **1**, 77 (1988).

[4] J.I. Pankov, *Mater. Res. Soc. Symp. Proc.* **97**, 409 (1987); J.I. Pankov, *Mater. Res. Soc. Symp. Proc.* **162**, 515 (1990).

[5] R. Riane, Z. Boussahla, A. Zaoui, L. Hammerlain, S.F. Matar, *Solid State Sci.* **11**, 200 (2009).

[6] J.A. VanVachten, T.K. Bergstresser, *Phys. Rev. B* **1**, 3351 (1970).

[7] D.J. Chadi, *Phys. Rev. B* **16**, 790 (1977).

[8] M. Rabah, B. Abbar, Y. Al-Douri, B. Bouhafs, B. Sahraoui, *Mater. Sci. Eng. B* **100**, 163 (2003).

[9] A. Baldereschi, K. Maschke, E. Hess, H. Neumann, K.-R. Schulze, K. Unger, *J. Phys. C* **10**, 4709 (1977).

[10] Z. Charifi, H. Baaziz, N. Bouarissa, *Int. J. Mod. Phys. B* **18**, 137 (2004); *Mater. Chem. Phys.* **84**, 273 (2004).

[11] A. Zaoui, *J. Phys., Condens. Matter* **14**, 4025 (2002).

[12] W. Sekkal, B. Bouhafs, H. Aourag, M. Certier, *J. Phys., Condens. Matter* **10**, 4975 (1998).

[13] R. Wentzcovitch, K.J. Chang, M.L. Cohen, *Phys. Rev. B* **34**, 1071 (1986).

[14] R. Wentzcovitch, M.L. Cohen, P.K. Lam, *Phys. Rev. B* **36**, 6058 (1987).

[15] P. Rodriguez-Hernandez, M. Gonzalez-Diaz, A. Munoz, *Phys. Rev. B* **51**, 14705 (1995).

[16] E. Knittle, R.M. Wentzcovitch, R. Jeanloz, M.L. Cohen, *Nature* (*London*) **337**, 349 (1989).

[17] O. Madelung, *Numerical Data and Functional Relationships in Science and Technology — Physics of Group IV Elements and III–V Compounds*, Landolt-Börnstein, Vol. 17, Springer, Berlin 1982.

[18] O. Madelung, *Numerical Data and Functional Relationships in Science and Technology — Crystal and Solid State Physics*, Vol. III, Landolt-Börnstein, Springer, Berlin 1972.

[19] V.A. Pesin, *Sverktverd Mater.* **6**, 5 (1980).

[20] P.E. Van Camp, V.E. Van Doren, J.T. Devreese, *Phys. Status Solidi B* **146**, 573 (1988).

[21] K. Karch, F. Bechstedt, *Phys. Rev. B* **56**, 7404 (1997).

[22] G.Q. Lin, H. Gong, P. Wu, *Phys. Rev. B* **71**, 085203 (2005).

[23] Z. Charifi, F. El Haj Hassan, H. Baaziz, Sh. Khosravizadeh, S.J. Hashemifar, H. Akbarzadeh, *J. Phys, Condens. Matter* **17**, 7077 (2005).

[24] S.H. Wei, A. Zunger, *Phys. Rev. B* **43**, 1662 (1991).

[25] S. Savrasov, D. Savrasov, *Phys. Rev. B* **46**, 12181 (1992).

[26] S.Y. Savrasov, *Phys. Rev. B* **54**, 16470 (1996).

[27] J.P. Perdew, Y. Wang, *Phys. Rev. B* **46**, 12947 (1992).

[28] P. Blaha, K. Schwarz, G.K.H. Madsen, D. Kvasnicka, J. Luitz, *WIEN2k, An Augmented-Plane-Wave + Local Orbitals Program for Calculating Crystal Properties*, Karlheinz Schwarz, Technische Universität Wien, Austria 2001.

[29] R. Dreizler, E.K.U. Gross, *Density-Functional Theory*, Springer, New York 1990.

[30] J.P. Perdew, S. Burke, M. Ernzerhof, *Phys. Rev. Lett.* **77**, 3865 (1996).

[31] J.P. Perdew, Y. Wang, *Phys. Rev. B* **67**, 235105 (2003).

[32] K. Schwarz, P. Blaha, *Comput. Mater. Sci.* **28**, 259 (2003).

[33] K. Schwarz, *J. Solid State Chem.* **176**, 319 (2003).

[34] G.H.K. Madsen, P. Blaha, K. Schwarz, E. Sjöstedt, L. Nordström, *Phys. Rev. B* **64**, 195134 (2001).

[35] G.H.K. Madsen, B.B. Iversen, P. Blaha, K. Schwarz, *Phys. Rev. B* **64**, 195102 (2001).

[36] D.D. Koelling, B.N. Harmon, *J. Phys. C* **10**, 3107 (1977).

[37] H.J. Monkhorst, J.D. Pack, *Phys. Rev. B* **13**, 5188 (1976).

[38] S. Larach, R.E. Shrader, C.F. Stocker, *Phys. Rev.* **108**, 587 (1957).

[39] A. Ebina, M. Yamamoto, T. Takahashi, *Phys. Rev. B* **6**, 3786 (1972).

[40] P. Blochl, O. Jepsen, O.K. Andersen, *Phys. Rev. B* **49**, 16223 (1994).

[41] L. Vegard, *Z. Phys.* **5**, 17 (1921).

[42] S.N. Rashkeev, W.R.L. Lambrecht, *Phys. Rev. B* **63**, 165212 (2001).

[43] F. El Haj Hassan, H. Akbarzadeh, *Mater. Sci. Eng. B* **21**, 170 (2005).

[44] Z. Dridi, B. Bouhafs, P. Ruterana, *Comput. Mater. Sci.* **33**, 136 (2005).

[45] A.M.N. Niklasson, J.M. Wills, M.I. Katsnelson, I.A. Abrikosov, O. Eriksson, B. Johannsson, *Phys. Rev. B* **38**, 7710 (1988).

[46] *Properties of Group III-Nitrides*, Ed. J.H. Edgar, EMIS Data Reviews **11**, INSPEC, London 1994, p. 10233.

[47] R. Del Sole, R. Girlanda, *Phys. Rev. B* **48**, 11789 (1993).

[48] F. Bechstedt, R. Del Sole, *Phys. Rev. B* **38**, 7710 (1988).

[49] Z. Boussahla, B. Abbar, B. Bouhafs, A. Tadjer, *J. Solid State Chem. B* **178**, 2117 (2005).

[50] C. Stampfl, C.G. Van de Walle, *Phys. Rev. B* **59**, 5521 (1999).

[51] A. Zaoui, F. ElhadiHassan, *J. Phys., Condens. Matter* **13**, 253 (2001).

[52] V.A. Fomichev, M.A. Rumsh, *J. Chem. Phys.* **48**, 555 (1968); V.A. Fomichev, M.A. Rumsh, *J. Chem. Phys.* **29**, 1015 (1968).

[53] *Numerical Data and Functional Relationships in Science and Technology, New Series*, Group III, Vol. 17, Part A, Springer, Berlin 1982.

[54] A. Trampert, O. Brandt, H.K. Ploog, in: *Crystal Structure of Group III-Nitrides, Semiconductors and Semimetals*, Vol. 50, Academic, San Diego 1998.

[55] M.E. Sherwin, T.J. Drumond, *J. Appl. Phys.* **69**, 8425 (1991).